DMD Fast Forward. Published on November 8, 2006 as doi:10.1124/dmd.106.012831
This article has not been copyedited and formatted. The final version may differ from this version.

DMD #012831

The *PXR*-humanized Mouse: A Model for Investigating Drug-drug Interactions Mediated by Cytochromes P450 3A

Xiaochao Ma, Yatrik Shah, Connie Cheung, Grace L. Guo, Lionel Feigenbaum, Kristopher W. Krausz, Jeffrey R. Idle, and Frank J. Gonzalez

Laboratory of Metabolism, Center for Cancer Research, National Cancer Institute, National Institutes of Health, Bethesda, MD 20892 (XM, YS, CC, KWK, FJG); Department of Pharmacology, Toxicology, and Therapeutics, University of Kansas Medical Center, Kansas City, KS 66160 (GLG); Laboratory Animal Science Program, SAIC, National Cancer Institute, Frederick, MD 21702 (LF); Institute of Pharmacology, 1st Faculty of Medicine, Charles University, 128 00 Praha 2, Czech Republic (JRI)

Running title: *PXR*-humanized mice and drug-drug interactions

Correspondence: Frank J. Gonzalez, Laboratory of Metabolism, Center for Cancer Research, National Cancer Institute, Building 37, Room 3106, Bethesda, MD 20892. Telephone: +301 496 9067. Fax: +301 496 8419. Email: fjgonz@helix.nih.gov

Number of text pages: 31

Number of tables: 1

Number of figures: 7

Number of references: 44

Number of words in the abstract: 223

Number of words the introduction: 725

Number of words the discussion: 1055

List of abbreviations: PXR: pregnane X receptor; CYP, cytochrome P450; BAC, bacterial artificial chromosome; hPXR, PXR-humanized transgenic mice; DDIs, drug-drug interactions; ADRs, adverse drug reactions; RXR, retinoid X receptor; RIF, rifampicin; PCN, pregnenolone 16α-carbonitrile; MDZ, midazolam; qPCR, quantitative real-time PCR; LC-MS/MS, liquid chromatography-coupled tandem mass spectrometry; *C*max, maximal serum concentration; AUC, area under the concentration-time curve.

DMD Fast Forward. Published on November 8, 2006 as DOI: 10.1124/dmd.106.012831
This article has not been copyedited and formatted. The final version may differ from this version.

Abstract

The most common clinical implication for the activation of the human pregnane X receptor (PXR) is the occurrence of drug-drug interactions mediated by up-regulated cytochrome P450 3A (CYP3A) isozymes. Typical rodent models do not predict drug-drug interactions mediated by human PXR, because of species differences in response to PXR ligands. In the current study, a *PXR*-humanized mouse model was generated by bacterial artificial chromosome (BAC) transgenesis in *Pxr*-null mice using a BAC clone containing the complete human *PXR* gene and 5' and 3' flanking sequence. In this *PXR*-humanized mouse model, PXR is selectively expressed in the liver and intestine, the same tissue expression pattern as CYP3A. Treatment of *PXR*-humanized mice with the PXR ligands mimicked the human response, as both hepatic and intestinal CYP3A were strongly induced by rifampicin, a human-specific PXR ligand, but not by pregnenolone 16α-carbonitrile, a rodent-specific PXR ligand. In rifampicin pretreated *PXR*-humanized mice, a ~60% decrease was observed for both the maximal midazolam serum concentration (C_{max}) and the area under the concentration-time curve (AUC), consequent upon a 3-fold increase in midazolam 1'-hydroxylation. These results illustrate the potential utility of the *PXR*-humanized mice in the investigation of drug-drug interactions mediated by CYP3A and suggest that the *PXR*-humanized mouse model would be an appropriate *in vivo* tool for the evaluation of the overall pharmacokinetic consequences of human PXR activation by drugs.

DMD Fast Forward. Published on November 8, 2006 as DOI: 10.1124/dmd.106.012831
This article has not been copyedited and formatted. The final version may differ from this version.

Introduction

Multiple-therapy regimens are commonly used in patients with cancer, HIV, cardiovascular disease, and diabetes. According to recent population-based surveys on drug use in the US, the highest overall prevalence of medication use was among patients aged over 65 years, of whom 12% took at least 10 medications and 50% took at least 5 medications (Kaufman et al., 2002). For patients with multiple drug exposure, drug-drug interactions (DDIs) have become an important issue in health care, which may decrease therapeutic efficacy and/or increase drug toxicity. A higher risk of adverse drug reactions (ADRs) were reported in patients receiving multiple drugs, which was proposed to be due to DDIs (May et al., 1977). Serious ADRs in patients require hospitalization, and some result in permanent disability or death (Lazarou et al., 1998). Therefore, understanding the mechanism of DDIs and the development of relevant animal models to predict DDIs in humans are both important goals for the improvement of drug safety.

Most DDIs are related to pharmacokinetics and result from interference of the metabolic clearance of one drug by a co-administered drug (Guengerich, 1997). Oral contraceptive failures are typical examples for DDIs which occur in women also receiving rifampicin or phenobarbital (D'Arcy, 1986). Induction of metabolic enzymes and increase in oral contraceptive clearance have been reported as the cause for oral contraceptive failures (Back and Orme, 1990). The cytochromes P450 (CYP) mainly involved in drug metabolism are found in the 1A, 2C, 2D and 3A subfamilies (Gonzalez, 1992). Of these, CYP3A4 is the most abundant P450 in the liver and participates in the metabolism of over 50% of clinically used drugs (Guengerich, 1999). There exist three minor CYP3A

enzymes, CYP3A5, CYP3A7, and CYP3A43 that also play a role in drug metabolism (Daly, 2006). Many common drugs such as the glucorticoid dexamethasone, the antibiotic rifampicin and the antimycotic clotrimazole, increase the expression of *CYP3A* genes as a result of transcriptional activation mediated by the pregnane X receptor (PXR; NR1I2), a member of the nuclear receptor superfamily. PXR is the dominant activator of *CYP3A* transcription and also plays an important role in regulating other genes involved in drug metabolism and elimination (Kliewer et al., 1998; Kliewer, 2005). Human PXR undergoes ligand activation and the resulting transcriptional activation of *CYP3A* involves the formation of a heterodimer with retinoid X receptor (RXR) which binds to PXR response elements in the 5' flanking region of the *CYP3A4* gene (Goodwin et al., 1999). Many clinical medicines have been identified as human PXR ligands (Honkakoski et al., 2003) including prescription drugs, herbal supplements, and vitamins. Thus, patients treated with combinations of drugs that are PXR ligands and are CYP3A substrates run the risk of DDIs.

An important concern is to identify whether drug candidates in development are PXR ligands and/or CYP3A substrates. Human liver microsomes and cDNA-expressed CYP3A4, together with CYP3A chemical inhibitors or CYP3A inhibitory antibodies, are common approaches to identify CYP3A substrates (Newton et al., 1995; Mei et al., 1999). Unfortunately, it is difficult to identify human PXR ligands due to important deficiencies in laboratory rodent models (Jones et al., 2000; Honkakoski et al., 2003). For example, drugs such as rifampicin, clotrimazole and troglitazone strongly activate human PXR but are weak activators of rodent PXR. In contrast, dexamethasone and pregnenolone 16α-

carbonitrile strongly activate rodent PXR but are weak activators of human PXR. Although cell-based reporter gene assays represent a simple and rapid *in vitro* tool for screening human PXR ligands and CYP3A inducers (Raucy et al., 2002), there remains the problem of extrapolating from *in vitro* results to the *in vivo* situation. Therefore, a *PXR*-humanized mouse model would be an ideal *in vivo* tool to study DDIs triggered by human PXR ligands. In previous studies, two humanized *PXR* mouse models, *Alb-VP-hPXR* and *FABP-VP-hPXR* transgenic mice, were generated by cDNA transgenesis (Xie et al., 2000; Gong et al., 2006). In the present study, a *PXR*-humanized mouse model was produced by bacterial artificial chromosome (BAC) transgenesis, in which the transgene contains the complete human *PXR* gene and the 5' and 3' flanking sequences. In this *PXR*-humanized mouse model, the role of human PXR on CYP3A induction was determined by pretreatment of mice with rifampicin and the investigation of midazolam, a prototypical CYP3A4 drug substrate, pharmacokinetics. This rifampicin/midazolam interaction illustrates the potential effectiveness of using this *PXR*-humanized mouse model in the study of DDIs mediated by CYP3A.

Materials and Methods

Chemicals. Rifampicin (RIF), pregnenolone 16α-carbonitrile (PCN), midazolam (MDZ), ketoconazole, and NADPH were obtained from Sigma-Aldrich (St. Louis MO). 1'-hydroxymidazolam (1'-OH-MDZ) was purchased from BD Gentest (Woburn, MA). All other chemicals were of the highest grade commercially available.

Generation of *PXR*-humanized transgenic mice. The BAC clone RP11-169N13 (Resgen/Invitrogen Corporation, Huntsville, AL) containing the complete human *PXR* gene sequence (Zhang et al., 2001), including 5' and 3' flanking sequence was purified by using a maxi prep kit (Qiagen, Valencia, CA). The BAC clone was verified initially by PCR using primers designed to amplify specific regions within exon 2 and 9, and the 5' UTR as described previously (Zhang et al., 2001). Additional verification of the BAC clone was carried out by Southern blot analysis with ^{32}P-end labeled human PXR cDNA (Lehmann et al., 1998) and DNA oligonucleotide probes recognizing specific regions (Exon 1 and 9, and -12.5 kb upstream) of the human *PXR* gene. The BAC clone was linearized by restriction enzyme digestion (P1-Sce) and purified before microinjection into fertilized FVB/N mouse eggs. Mice resulting from this breeding step that were positive for the human *PXR* transgene by PCR analysis were bred further with *Pxr*-null mice (Staudinger et al., 2001) kindly provided by GlaxoSmithKline Inc., and Dr. Steven A. Kliewer (Dallas,TX). Mice positive for the human *PXR* transgene and the *Pxr* null allele, as determined by PCR genotyping, were designated as *PXR*-humanized transgenic (hPXR) mice. The hPXR mice were further bred with *Pxr*-null mice for at least 4 generations onto C57BL/6 background. Mice heterozygous for hPXR transgene were then bred interbred to generate a homozygous

line that was confirmed to be homzygous by breeding wild-type mice; all the litters were positive for hPXR.

Animals and treatments. Male, 2 to 4-month-old hPXR, *Pxr*-null and wild-type (WT) mice, were maintained under a standard 12 h light/12 h dark cycle with water and chow provided *ad libitum*. The WT mouse background is C57BL/6. Handling was in accordance with animal study protocols approved by the National Cancer Institute Animal Care and Use Committee. For CYP3A induction, WT and *Pxr*-null and hPXR mice were injected *i.p.* with 10 mg/kg/day PCN, or *p.o.* with 10 mg/kg/day RIF, daily for 3 days. All mice were sacrificed by CO_2 asphyxiation 24 h after the last dose. Liver and small intestine were collected and frozen at -80 °C for further analysis. To detect CYP3A expression after the withdrawal of PXR ligand, the hPXR mice were treated with RIF (10 mg/kg/day) for 3 days. 1, 2, 4, 6, 8, and 10 days following the last dose, mouse liver and small intestine were collected and frozen at -80 °C for CYP3A expression analysis.

PCR genotyping. The presence of the human *PXR* transgene was determined using the following primers, *hPXR* 5' UTR Fwd: 5'- GCA CCT GCT GCT AGG GAA TA-3' and *hPXR* 5' UTR Rev: 5'- CTC CAT TGC CCC TCC TAA GT-3' amplifying a PCR product of 576 bp in only the samples positive for this transgene. Mouse epoxide hydrolase 1 gene (*Ephx1*) primers served as an internal positive control for amplification, yielding a fragment of 341 bp in all samples (Miyata et al., 1999). The following primers were used to identify the mouse *PXR* WT and null alleles, PXR-Fwd1: 5'- CTG GTC ATC ACT GTT GCT GTA CCA-3', PXR-Rev2: 5'- GCA GCA TAG GAC AAG TTA TTC TAG AG-3'

and PXR-Rev3 : 5'- CTA AAG CGC ATG CTC CAG ACT GC-3' amplifying a PCR product of 348 bp for WT allele and 265 bp for *Pxr*-null allele (Guo et al., 2003).

Southern blot analysis. To analyze the BAC clone, DNA was digested with *Eco*RI, *Sac*I, *Bgl*II, *Nco*I or *Afl*II. Electrophoresis and southern hybridization conditions were described previously (Granvil et al., 2003). Random-primer ^{32}P-labelled human PXR cDNA and DNA oligonucleotide probes recognizing specific regions of the human *PXR* gene were used for analysis of the BAC clone.

RNA analysis. Human PXR tissue distribution in hPXR mice was analyzed by quantitative real-time PCR (qPCR). RNA was extracted from different tissues using TRIzol reagent (Invitrogen, Carlsbad, CA). qPCR was performed using cDNA generated from 1µg total RNA with SuperScript II Reverse Transcriptase kit (Invitrogen). Primers were designed for qPCR using the Primer Express software (Applied Biosystems). hPXR: Fwd: 5'-GGC CAC TGG CTA TCA CTT CAA-3'; Rev: 5'-TTC ATG GCC CTC CTG AAA A-3'. mPXR: Fwd: 5'-AAG AAG CAG ACT CTG CCT TGG A-3'; Rev: 5'-GTG GTA GCC ATT GGC CTT GT-3'. CYP3A11: Fwd: 5'-AGC AGG GAT GGA CCT GG-3'; Rev: 5'-CGG TAG AGG AGC ACC AA-3'. qPCR reactions were carried out using SYBR green PCR master mix (SuperArray) in an ABI Prism 7900HT Sequence Detection System (Applied Biosystems, Foster City, CA). Values were quantified using the Comparative CT method, and samples normalized to β-actin.

Microsome preparation and western blot analysis. Liver and small intestine were homogenized in ice-cold buffer (50 mM Tris–HCl, 150 mM KCl, 1 mM EDTA and 20% glycerol). Microsomes were prepared by centrifugation at 10,000 *g* for 20 min at 4°C, and the resulting supernatant spun at 100,000 *g* for 1 hr at 4°C. Microsomal pellets were resuspended in the same ice-cold buffer used for homogenization. For western blot analysis, microsomal protein (10 µg) from each sample was separated by SDS-PAGE, electrophoretically transferred to nitrocellulose membranes (Schleicher & Schuell, Keene, NH), and probed using anti-rat CYP1A2 mAb (clone 22-341), anti-rat CYP2C polyclonal Ab, anti-rat CYP2D polyclonal Ab, anti-rat CYP2E1 mAb (clone 1-98-1), anti-rat CYP3A1/2 mAb (clone 2-13-1), and anti-GAPDH polyclonal Ab (Chemicon International, Temecula, CA). Secondary antibodies, goat anti-mouse IgG (Cat 115-036-071) and goat anti-rabbit IgG (Cat 111-036-045), were purchased from Jackson ImmunoResearch Laboratories, Inc (West Grove, PA). Detection of immunoreactive proteins was done by an enhanced chemiluminescence blot detection system (Amersham Biosciences).

CYP3A activity analysis. Midazolam 1'-hydroxylation was used as a probe for CYP3A activity (Thummel et al., 1994). The incubation was performed in 100 mM sodium phosphate buffer (pH 7.4) containing microsomes with 50 to 100 µg of protein, and 50 µM MDZ in a final volume of 200 µl. For the inhibitory analysis, 2 µM ketoconazole (final concentration) was added in the incubation system and pre-incubated at 37°C for 5 min. The reaction was initiated by the addition of 20 µl of 20 mM NADPH, 37°C for 10 min, and terminated by the addition of 1 ml ethyl acetate and 1 ml methyl *t*-butyl ether mixture. Samples were centrifuged at 3,000 rpm for 5 min at 4 °C. The organic layer was then

transferred to a new tube, dried with N_2 and reconstituted in 100 µl of 70% methanol and 30% H_2O containing 0.1% formic acid. All reactions were performed in duplicate. 1'-OH-MDZ was detected by liquid chromatography-coupled tandem mass spectrometry (LC-MS/MS).

Pharmacokinetic study of midazolam in hPXR mice. WT and hPXR mice were pretreated with or without 10 mg/kg RIF, once daily for 3 days. 24 h after the last dose of RIF, mice were administered with 5 mg/kg MDZ orally by gavage. Blood samples were collected from suborbital veins using heparinized tubes at 0, 5, 10, 20, 30, 60, 90, 120, and 180 min after administration of MDZ. Serum was separated by centrifugation at 8,000 *g* for 10 min. For MDZ extraction, 50 µl serum was mixed with 150 µl PBS, 200 µl ethyl acetate and 200 µl methyl *t*-butyl ether. The mixture was centrifuged at 3,000 rpm for 5 min at 4 °C. The organic layer was then transferred to a new tube, dried with N_2 and reconstituted in 100 µl of 70% methanol and 30% H_2O containing 0.1% formic acid. MDZ and 1'-OH-MDZ were detected by LC-MS/MS. Pharmacokinetic parameters for MDZ were estimated from the plasma concentration-time data by a non-compartmental approach using WinNonlin (Pharsight, Mountain View, CA). The maximum concentration in serum (C_{max}) was obtained from the original data. The area under the serum concentration-time curve ($AUC_{0\text{-}180\ min}$) was calculated by the trapezoidal rule.

Analysis of midazolam and 1'-OH-midazolam by LC-MS/MS. MDZ and its metabolites 1'-OH-MDZ were determined by LC-MS/MS based on a previous method (Granvil et al., 2003) with minor modifications. LC-MS/MS analysis was carried out using a high-

performance liquid chromatography system consisting of a PerkinElmer Series 200 quaternary pump, vacuum degasser, and autosampler with a 100 µl loop interfaced to an API2000 SCIEX triple-quadrupole tandem mass spectrometer (Applied Biosystems/MDS Sciex, Foster City, CA). MDZ, 1'-OH-MDZ, and 6-chloromelatonin (internal standard) were separated on a Luna C18 50 mm x 4.6 mm *i.d.* column (Phenomenex, Torrance, CA). The flow rate through the column at ambient temperature was 0.25 ml/min with 70% methanol and 30% H_2O containing 0.1% formic acid. Each analysis lasted for 5.0 min. The mass spectrometer was operated in the turbo ion spray mode with positive ion detection. The turbo ion spray temperature was maintained at 300 °C, and a voltage of 4.8 kV was applied to the sprayer needle. N_2 was used as the turbo ion spray and nebulizing gas. The detection and quantification of analysts were performed using the multiple reactions monitoring (MRM) mode, with m/z 326/291 for MDZ, m/z 342/203 for 1-OH-MDZ, and m/z 267/208 for 6-chloromelatonin.

Statistical analysis. All values are expressed as the means ± SD and group differences analyzed by unpaired Student's *t* test.

DMD Fast Forward. Published on November 8, 2006 as DOI: 10.1124/dmd.106.012831
This article has not been copyedited and formatted. The final version may differ from this version.

Results

Generation of *PXR*-humanized mice. A transgenic mouse line was created using a BAC clone containing the complete human *PXR* gene sequence and including 5' and 3' flanking sequence (Fig. 1A). The BAC clone was verified initially by PCR using primers designed to amplify specific regions within exon 2 and 9, and the 5' UTR (Fig. 1B). Additional verification of the BAC clone was carried out by Southern blot analysis with ^{32}P-end labeled human PXR cDNA and DNA oligonucleotide probes recognizing specific regions (Exon 1 and 9, and -12.5 kb upstream) of the human *PXR* gene. The size of each hybridized band corresponded well with the size predicted from the map of the human *PXR* gene sequence (Data not shown). The BAC clone was linearized by restriction enzyme digestion and purified before microinjection into fertilized FVB/N mouse eggs. Several transgenic founders were identified by Southern blot analysis and bred with *Pxr*-null mice. Mice which were positive for the human *PXR* transgene and containing the mouse *Pxr*-null allele, as determined by PCR genotyping (Fig. 1C), were bred to generate homozygous mice and designated as *PXR*-humanized transgenic (hPXR) mice.

PXR tissue distribution. PXR tissue distribution was analyzed by qPCR. Human PXR was detected in hPXR mice in liver, duodenum, jejunum, and ileum, but not in lung and heart (Fig. 2A). Similar tissue distribution was reported in humans, however the expression level of PXR in human liver is much higher when compared to the intestinal tract (Bertilsson et al., 1998; Blumberg et al., 1998; Lehmann et al., 1998). PXR expression in the mouse liver was shown to be similar to PXR expression levels in the intestinal tract (Jones et al., 2000). In this hPXR mouse model, human PXR expression

levels were similar in liver and gut, a finding analogous to that of mouse PXR expression in WT mice (Fig. 2B).

CYP3A expression and regulation in hPXR mice. In the hPXR mouse model, human PXR is selectively expressed in the liver and intestine, the same tissues that express CYP3A. Xenobiotic response of CYP3A in hPXR mice was analyzed by qPCR (Fig. 3A) and Western blot (Fig. 3B). In hPXR mice, CYP3A11 mRNA and CYP3A protein was strongly induced by RIF, a human-specific PXR ligand, but not by PCN, a rodent-specific PXR ligand. In WT mice, CYP3A11 mRNA was strongly induced by PCN, but not by RIF. Neither PCN nor RIF resulted in significant CYP3A11 induction in *Pxr*-null mice. Following the withdrawal of RIF treatment in hPXR mice, hepatic CYP3A protein expression was still remarkably high, and it took about one week to return to the basal level (Fig. 4A). These data indicated that DDIs may still occur in patients who take drugs that are CYP3A substrates soon after withdrawal of drugs that are PXR ligands. The importance of intestinal CYP3A in drug metabolism was addressed in a previous study using a transgenic *CYP3A4* mouse model (Granvil et al., 2003). In the hPXR mouse model, induction of intestinal CYP3A protein was also noted, which increased significantly after 3 days of treatment with RIF. Compared to hepatic CYP3A, intestinal CYP3A expression decreased more rapidly after withdrawal of ligand (Fig. 4B). Other hepatic P450s were also investigated, however no significant effect was observed on the expression of hepatic CYP1A2, CYP2C, CYP2D, and CYP2E1 P450s in a constitutively-activated hPXR mouse line (Fig. 5). In a previous report on another line of PXR-humanized mice (VP-hPXR), CYP2C mRNAs were not induced by RIF (Rosenfeld et al., 2003). The lack

of CYP2C induction is of interest since in cultured human hepatocytes, RIF induced CYP2C mRNAs (Raucy et al., 2002; Ferguson et al., 2005). However, earlier studies in mice did not reveal induction of CYP2C transcripts with the rodent PXR ligand PCN (Guzelian et al., 2006; Jackson et al., 2006). These results suggest the possibility of a species difference in PXR-binding elements controlling *CYP2C* genes.

CYP3A activity and pharmacokinetic study of midazolam in hPXR mice. *In vitro* hepatic CYP3A activity was analyzed by using midazolam 1'-hydroxylase as a probe (Thummel et al., 1994). Consistent with CYP3A expression, CYP3A activity increased significantly in hPXR mice treated with RIF. In WT and *Pxr*-null mice, RIF produced no significant effect on CYP3A activity (Fig. 6A and Fig. 6B). In hPXR mice treated with RIF, CYP3A activity increased 314% compared to the vehicle treated control (Fig. 6C). CYP3A activity in hPXR mice following RIF treatment was significantly inhibited (~90%) by ketoconazole (KCZ) at 2 μM (Fig. 6D). *In vivo*, MDZ and RIF interactions were investigated in WT and hPXR mice. MDZ is a short-acting hypnotic-sedative drug metabolized by CYP3A (Gorski et al., 1994). Loss of the pharmacodynamic effects of MDZ was noted in tuberculosis patients undergoing RIF treatment and human PXR activation and CYP3A induction were proposed as key factors in this DDI (Backman et al., 1996; Niemi et al., 2003). This clinical phenomenon was recapitulated and illuminated by using the hPXR mouse model. In WT mice, RIF has no significant effect on MDZ pharmacokinetics (Fig. 7A and Table 1). However, in hPXR mice pretreated with RIF, the maximal MDZ serum concentration (C_{max}) was decreased by 64% and the area under the concentration-time curve ($AUC_{0\text{-}180\ min}$) was decreased by 60% (Fig 7B and Table 1).

Discussion

In the current study, a humanized PXR mouse model was generated by BAC transgenesis in *Pxr*-null mice, and contained the complete human *PXR* gene, including the 5' and 3' flanking sequences. In the hPXR mouse model, PXR was selectively expressed in the liver and intestine, the same tissue expression pattern as CYP3A. Treatment with PXR ligands showed a clear species difference in response to xenobiotics between WT and hPXR mice, which suggests that this BAC transgenic hPXR mouse model is useful for the investigation of human PXR function *in vivo*.

PXR, a member of the nuclear receptor superfamily, plays an important role in regulating CYP3A and other genes involved in drug metabolism and elimination (Kliewer, 2005). The most common clinical implication of human PXR activation is the occurrence of DDIs. This is because CYP3A P450s, predominantly CYP3A4, metabolize over 50% of clinically used drugs. This phenomenon is ably illustrated by RIF, where hundreds of drugs have been reported to result in DDIs during combined therapy with RIF (Niemi et al., 2003). RIF, a first-line antitubercular drug, has been used for over 40 years, and DDIs with RIF were noted soon after its clinical introduction, such as the interaction between RIF and oral contraceptives (Rocher et al., 1971). However, for drugs in development, it is difficult to predict using rodents the likely occurrence of clinical drug interactions with RIF. This is due to species differences between rodents and humans in the response to PXR ligands (Jones et al., 2000; LeCluyse, 2001; Tirona et al., 2004). Therefore, the employment of a hPXR mouse model would provide a solution to this problem through the expression of the human receptor in mouse liver and intestine.

High-throughput *in vitro* PXR activation and binding assays have been employed to identify PXR ligands and CYP3A inducers, and it was concluded that the PXR reporter gene assay is a reliable and complementary method to evaluate CYP3A induction (Luo et al., 2002; Zhu et al., 2004). However, the general problem remains, that of extrapolating from *in vitro* findings to the clinical situation *in vivo*. It has been speculated that a *PXR*-humanized mouse model might be informative regarding human DDIs (Xie and Evans, 2002). A previously reported hPXR mouse model, *Alb-VP-hPXR*, was generated expressing a constitutively active human PXR in the liver of *Pxr*-null mice (Xie et al., 2000). The limit of this hPXR mouse model was hepatic specific PXR expression, which did not reflect the full characteristics of human PXR, especially for its role in gut. The hPXR mouse model generated by BAC transgenesis in the current study showed PXR expression and CYP3A induction both in liver and gut. Investigation of the metabolism and pharmacokinetics of MDZ illustrated the potential effectiveness of using the hPXR mice for the study the induction of CYP3A and thus its associated DDIs. The interaction between RIF and MDZ could not have been predicted from studies in WT mice because murine PXR is not activated by RIF (see Fig. 3). We take the interaction between RIF and MDZ in hPXR mice to be a paradigm for clinical interactions between PXR ligand drugs and CYP3A substrates. Not all drug metabolism mediated by CYP3A P450s can be attributed to the predominant form CYP3A4. About 20% of human livers express CYP3A5 and the occurrence of the WT *CYP3A5*1* allele displays considerable interethnic heterogeneity (Daly, 2006). Moreover, CYP3A5 is thought to account for 17% to 50% of hepatic CYP3A protein and this may also be the same for intestinal CYP3A5. It would

also appear from pharmacogenetic studies that CYP3A5 may contribute little if anything to the metabolism of classical CYP3A4 substrates, such as midazolam, cyclosporine, nifedipine and docetaxel (Daly, 2006). However, for the immunosuppressant drug tacrolimus, multiple reports have established that CYP3A5 is a major contributor to its metabolism (Daly, 2006). The tissue distribution, induction and clinical relevance of the minor P450 forms CYP3A7 and CYP3A43 remain more poorly understood. Nevertheless, clinical interactions between drugs that are PXR ligands and drugs that are CYP3A4, CYP3A5, CYP3A7, and CYP3A43 substrates would be expected to be predicted from the hPXR mouse model.

An earlier hPXR model (Xie et al., 2000) has been employed to study the role of the P-glycoprotein export pump in the blood-brain barrier. P-glycoprotein provides a principal mechanism by which drugs are excluded from the brain. While the plasma levels of methadone in control and RIF-induced hPXR mice were similar, the antinociceptive effects of methadone were about 70% reduced in the RIF-induced hPXR mice (Bauer et al., 2006). In addition to characterizing an important interaction between RIF and methadone, at the level of PXR, this report also demonstrates that PXR expression in the blood-brain barrier in hPXR mice can also induce expression of P-glycoprotein through regulation by PXR of the *MDR1* (*ABCB1*) gene (Bauer et al., 2006). This represents another potential application of hPXR mice in drug development, the identification of PXR ligands that may exclude drugs from the brain via the induction of brain capillary P-glycoprotein. It will be possible therefore to evaluate this model for its combined utility in the prediction of pharmacokinetic drug-drug interactions at the level of both metabolism and transport.

Although a vast number of CYP3A substrates is known, less is understood about the ability of drugs to act as PXR ligands and thus induce hepatic and gut CYP3A activity and P-glycoprotein in the blood-brain barrier. It has been speculated that the development of new PXR ligands might be avoided through appropriate *in silico* screening procedures (Ekins and Erickson, 2002). Because the ligand binding domain of PXR is large and flexible, this permits a diverse range of ligands to interact with PXR. It is therefore reasonable to consider every new drug candidate in preclinical development as a potential PXR ligand, with the undesirable effects on both drug metabolism and distribution. A pharmacophore for human PXR ligands has been developed and tested and was able to distinguish the most potent PXR activators from weaker ones (Ekins and Erickson, 2002). The final test of a novel human PXR ligand would be to test it in the hPXR mouse model described here to evaluate its potential for causing drug-drug interactions in the clinic.

In conclusion, a *PXR*-humanized mouse model was generated successfully by BAC transgenesis, and it may become a useful tool for the investigation and prediction of pharmacokinetic DDIs.

References

Back DJ and Orme ML (1990) Pharmacokinetic drug interactions with oral contraceptives. *Clin Pharmacokinet* **18:**472-484.

Backman JT, Olkkola KT and Neuvonen PJ (1996) Rifampin drastically reduces plasma concentrations and effects of oral midazolam. *Clin Pharmacol Ther* **59:**7-13.

Bauer B, Yang X, Hartz AM, Olson ER, Zhao R, Kalvass JC, Pollack GM and Miller DS (2006) In vivo activation of human PXR tightens the blood-brain barrier to methadone through P-glycoprotein upregulation. *Mol Pharmacol*.

Bertilsson G, Heidrich J, Svensson K, Asman M, Jendeberg L, Sydow-Backman M, Ohlsson R, Postlind H, Blomquist P and Berkenstam A (1998) Identification of a human nuclear receptor defines a new signaling pathway for CYP3A induction. *Proc Natl Acad Sci U S A* **95:**12208-12213.

Blumberg B, Sabbagh W, Jr., Juguilon H, Bolado J, Jr., van Meter CM, Ong ES and Evans RM (1998) SXR, a novel steroid and xenobiotic-sensing nuclear receptor. *Genes Dev* **12:**3195-3205.

D'Arcy PF (1986) Drug interactions with oral contraceptives. *Drug Intell Clin Pharm* **20:**353-362.

Daly AK (2006) Significance of the minor cytochrome P450 3A isoforms. *Clin Pharmacokinet* **45:**13-31.

Ekins S and Erickson JA (2002) A pharmacophore for human pregnane X receptor ligands. *Drug Metab Dispos* **30:**96-99.

Ferguson SS, Chen Y, LeCluyse EL, Negishi M and Goldstein JA (2005) Human CYP2C8 is transcriptionally regulated by the nuclear receptors constitutive androstane

receptor, pregnane X receptor, glucocorticoid receptor, and hepatic nuclear factor 4alpha. *Mol Pharmacol* **68:**747-757.

Gong H, Singh SV, Singh SP, Mu Y, Lee JH, Saini SP, Toma D, Ren S, Kagan VE, Day BW, Zimniak P and Xie W (2006) Orphan nuclear receptor pregnane X receptor sensitizes oxidative stress responses in transgenic mice and cancerous cells. *Mol Endocrinol* **20:**279-290.

Gonzalez FJ (1992) Human cytochromes P450: problems and prospects. *Trends Pharmacol Sci* **13:**346-352.

Goodwin B, Hodgson E and Liddle C (1999) The orphan human pregnane X receptor mediates the transcriptional activation of CYP3A4 by rifampicin through a distal enhancer module. *Mol Pharmacol* **56:**1329-1339.

Gorski JC, Hall SD, Jones DR, VandenBranden M and Wrighton SA (1994) Regioselective biotransformation of midazolam by members of the human cytochrome P450 3A (CYP3A) subfamily. *Biochem Pharmacol* **47:**1643-1653.

Granvil CP, Yu AM, Elizondo G, Akiyama TE, Cheung C, Feigenbaum L, Krausz KW and Gonzalez FJ (2003) Expression of the human CYP3A4 gene in the small intestine of transgenic mice: in vitro metabolism and pharmacokinetics of midazolam. *Drug Metab Dispos* **31:**548-558.

Guengerich FP (1997) Role of cytochrome P450 enzymes in drug-drug interactions. *Adv Pharmacol* **43:**7-35.

Guengerich FP (1999) Cytochrome P-450 3A4: regulation and role in drug metabolism. *Annu Rev Pharmacol Toxicol* **39:**1-17.

Guo GL, Lambert G, Negishi M, Ward JM, Brewer HB, Jr., Kliewer SA, Gonzalez FJ and Sinal CJ (2003) Complementary roles of farnesoid X receptor, pregnane X receptor, and constitutive androstane receptor in protection against bile acid toxicity. *J Biol Chem* **278:**45062-45071.

Guzelian J, Barwick JL, Hunter L, Phang TL, Quattrochi LC and Guzelian PS (2006) Identification of Genes Controlled by the Pregnane X Receptor by Microarray Analysis of mRNAs from Pregnenolone 16{alpha}-carbonitrile Treated Rats. *Toxicol Sci*.

Honkakoski P, Sueyoshi T and Negishi M (2003) Drug-activated nuclear receptors CAR and PXR. *Ann Med* **35:**172-182.

Jackson JP, Ferguson SS, Negishi M and Goldstein JA (2006) Phenytoin Induction of the Cyp2c37 Gene is Mediated by the Constitutive Androstane Receptor. *Drug Metab Dispos*.

Jones SA, Moore LB, Shenk JL, Wisely GB, Hamilton GA, McKee DD, Tomkinson NC, LeCluyse EL, Lambert MH, Willson TM, Kliewer SA and Moore JT (2000) The pregnane X receptor: a promiscuous xenobiotic receptor that has diverged during evolution. *Mol Endocrinol* **14:**27-39.

Kaufman DW, Kelly JP, Rosenberg L, Anderson TE and Mitchell AA (2002) Recent patterns of medication use in the ambulatory adult population of the United States: the Slone survey. *Jama* **287:**337-344.

Kliewer SA (2005) Pregnane X receptor: predicting and preventing drug interactions. *Thromb Res* **117:**133-136; discussion 145-151.

Kliewer SA, Moore JT, Wade L, Staudinger JL, Watson MA, Jones SA, McKee DD, Oliver BB, Willson TM, Zetterstrom RH, Perlmann T and Lehmann JM (1998) An orphan nuclear receptor activated by pregnanes defines a novel steroid signaling pathway. *Cell* **92:**73-82.

Lazarou J, Pomeranz BH and Corey PN (1998) Incidence of adverse drug reactions in hospitalized patients: a meta-analysis of prospective studies. *Jama* **279:**1200-1205.

LeCluyse EL (2001) Pregnane X receptor: molecular basis for species differences in CYP3A induction by xenobiotics. *Chem Biol Interact* **134:**283-289.

Lehmann JM, McKee DD, Watson MA, Willson TM, Moore JT and Kliewer SA (1998) The human orphan nuclear receptor PXR is activated by compounds that regulate CYP3A4 gene expression and cause drug interactions. *J Clin Invest* **102:**1016-1023.

Luo G, Cunningham M, Kim S, Burn T, Lin J, Sinz M, Hamilton G, Rizzo C, Jolley S, Gilbert D, Downey A, Mudra D, Graham R, Carroll K, Xie J, Madan A, Parkinson A, Christ D, Selling B, LeCluyse E and Gan LS (2002) CYP3A4 induction by drugs: correlation between a pregnane X receptor reporter gene assay and CYP3A4 expression in human hepatocytes. *Drug Metab Dispos* **30:**795-804.

May FE, Stewart RB and Cluff LE (1977) Drug interactions and multiple drug administration. *Clin Pharmacol Ther* **22:**322-328.

Mei Q, Tang C, Assang C, Lin Y, Slaughter D, Rodrigues AD, Baillie TA, Rushmore TH and Shou M (1999) Role of a potent inhibitory monoclonal antibody to cytochrome P-450 3A4 in assessment of human drug metabolism. *J Pharmacol Exp Ther* **291:**749-759.

Miyata M, Kudo G, Lee YH, Yang TJ, Gelboin HV, Fernandez-Salguero P, Kimura S and Gonzalez FJ (1999) Targeted disruption of the microsomal epoxide hydrolase gene. Microsomal epoxide hydrolase is required for the carcinogenic activity of 7,12-dimethylbenz[a]anthracene. *J Biol Chem* **274:**23963-23968.

Newton DJ, Wang RW and Lu AY (1995) Cytochrome P450 inhibitors. Evaluation of specificities in the in vitrometabolism of therapeutic agents by human liver microsomes. *Drug Metab Dispos* **23:**154-158.

Niemi M, Backman JT, Fromm MF, Neuvonen PJ and Kivisto KT (2003) Pharmacokinetic interactions with rifampicin: clinical relevance. *Clin Pharmacokinet* **42:**819-850.

Raucy J, Warfe L, Yueh MF and Allen SW (2002) A cell-based reporter gene assay for determining induction of CYP3A4 in a high-volume system. *J Pharmacol Exp Ther* **303:**412-423.

Raucy JL, Mueller L, Duan K, Allen SW, Strom S and Lasker JM (2002) Expression and induction of CYP2C P450 enzymes in primary cultures of human hepatocytes. *J Pharmacol Exp Ther* **302:**475-482.

Rocher G, Haour P, Viallier J, Bouvy F and Van Theemsche G (1971) [Rifampicin, pregnancy, hormonal contraception, menopause and aging]. *Rev Tuberc Pneumol (Paris)* **35:**695-712.

Rosenfeld JM, Vargas R, Jr., Xie W and Evans RM (2003) Genetic profiling defines the xenobiotic gene network controlled by the nuclear receptor pregnane X receptor. *Mol Endocrinol* **17:**1268-1282.

Staudinger JL, Goodwin B, Jones SA, Hawkins-Brown D, MacKenzie KI, LaTour A, Liu Y, Klaassen CD, Brown KK, Reinhard J, Willson TM, Koller BH and Kliewer SA

(2001) The nuclear receptor PXR is a lithocholic acid sensor that protects against liver toxicity. *Proc Natl Acad Sci U S A* **98:**3369-3374.

Thummel KE, Shen DD, Podoll TD, Kunze KL, Trager WF, Hartwell PS, Raisys VA, Marsh CL, McVicar JP, Barr DM and et al. (1994) Use of midazolam as a human cytochrome P450 3A probe: I. In vitro-in vivo correlations in liver transplant patients. *J Pharmacol Exp Ther* **271:**549-556.

Tirona RG, Leake BF, Podust LM and Kim RB (2004) Identification of amino acids in rat pregnane X receptor that determine species-specific activation. *Mol Pharmacol* **65:**36-44.

Xie W, Barwick JL, Downes M, Blumberg B, Simon CM, Nelson MC, Neuschwander-Tetri BA, Brunt EM, Guzelian PS and Evans RM (2000) Humanized xenobiotic response in mice expressing nuclear receptor SXR. *Nature* **406:**435-439.

Xie W and Evans RM (2002) Pharmaceutical use of mouse models humanized for the xenobiotic receptor. *Drug Discov Today* **7:**509-515.

Zhang J, Kuehl P, Green ED, Touchman JW, Watkins PB, Daly A, Hall SD, Maurel P, Relling M, Brimer C, Yasuda K, Wrighton SA, Hancock M, Kim RB, Strom S, Thummel K, Russell CG, Hudson JR, Jr., Schuetz EG and Boguski MS (2001) The human pregnane X receptor: genomic structure and identification and functional characterization of natural allelic variants. *Pharmacogenetics* **11:**555-572.

Zhu Z, Kim S, Chen T, Lin JH, Bell A, Bryson J, Dubaquie Y, Yan N, Yanchunas J, Xie D, Stoffel R, Sinz M and Dickinson K (2004) Correlation of high-throughput pregnane X receptor (PXR) transactivation and binding assays. *J Biomol Screen* **9:**533-540.

Footnotes

This work was supported by the NCI Intramural Research Program, and in part by NIH (NIAID) grant U19 AI067773-02. JRI is grateful to U.S. Smokeless Tobacco Company for a grant for collaborative research. The authors thank John R. Buckley for technical assistance.

Figure Legends

Fig. 1 Generation and genetic characterization of *PXR*-humanized mice. (**A).** Structure of the BAC clone containing the complete human *PXR* gene sequence (exons 1-9) and the 5' and 3' flanking sequences. (**B**). Verification of the BAC clone by PCR using primers designed to amplify specific regions within exon 2 and 9, and the 5' UTR. (**C**). A representative genotyping result for hPXR mice. Mouse epoxide hydrolase 1 gene (*Ephx1*) primers served as an internal positive control. Mouse lines 4 and 5 were positive for the human *PXR* transgene and containing the mouse *Pxr*-null allele.

Fig. 2 PXR tissue distribution in wild-type and *PXR*-humanized mice. PXR tissue distribution was analyzed by qPCR. (**A**) Human PXR tissue distribution in *PXR*-humanized mice. (**B**) Mouse PXR tissue distribution in WT mice. Values were quantified using the Comparative CT method, and samples normalized to β-actin.

Fig. 3 Hepatic CYP3A expression and regulation in *PXR*-humanized mice. Animals were treated with PXR ligands, RIF or PCN, 10 mg/kg/day for 3 days. (A) qPCR analysis of CYP3A11 expression. Values were quantified using the Comparative CT method, and samples normalized to β-actin. (B) Western blot analysis of mouse CYP3A, GAPDH served as a loading control.

Fig. 4 CYP3A expression in liver and intestine of *PXR*-humanized mice after the withdrawal of RIF treatment. hPXR mice were treated with RIF, 10 mg/kg/day for 3 days. CYP3A was detected by western blot, GAPDH served as a loading control. (A) CYP3A

expression in liver after the withdrawal of RIF treatment. (B) CYP3A expression in small intestine (S. Intestine) after the withdrawal of RIF treatment.

Fig. 5 Effect of human PXR ligand treatment on the expression of major CYP isoenzymes in *PXR*-humanized mice. hPXR mice were treated with RIF, 10 mg/kg/day for 3 days. CYP1A2, 2C, 2D, 2E1, and 3A were detected by western blotting. GAPDH served as a loading control.

Fig. 6 CYP3A activity analysis in liver microsomes of WT, *Pxr*-null, and *PXR*-humanized mice, treated with RIF, 10 mg/kg/day for 3 days. Midazolam 1'-hydroxylation was used as the probe for CYP3A activity, and analyzed by LC-MS/MS. CYP3A activity in control group was set as 100% for each animal line. Data were expressed as means ± SD, n=3. (**A**) CYP3A activity in WT mice. (**B**) CYP3A activity in *Pxr*-null mice. (**C**) CYP3A activity in hPXR mice. **P*< 0.01 compared with control. (**D**) Inhibition on CYP3A activity by ketoconazole (KCZ) in hPXR mice with RIF pretreatment. **P*< 0.01 compared with no KCZ group.

Fig. 7 Effect of RIF on midazolam pharmacokinetics in WT and *PXR*-humanized mice. hPXR mice and WT mice were pretreated with RIF, 10 mg/kg/day for 3 days. (**A**) Time course of serum MDZ in WT mice with or without RIF pre-treatment. (**B**) Time course of serum MDZ in hPXR mice with or without RIF pre-treatment.

DMD Fast Forward. Published on November 8, 2006 as DOI: 10.1124/dmd.106.012831
This article has not been copyedited and formatted. The final version may differ from this version.

Table 1 Pharmacokinetics of midazolam (MDZ) in wild-type and *PXR*-humanized mice, pretreated with or without RIF, at 10 mg/kg/day for 3 days. Serum MDZ was detected by LC-MS/MS. Pharmacokinetic parameters were estimated from the serum concentration-time (3 mice at each time point) data by a noncompartmental approach using WinNonlin. Data were expressed as means ± SD.

Genotype	MDZ	Control	RIF	RIF (% control)
Wild-type	C_{max} (nmol/l)	1085±50	908±3	83.6
	AUC_{0-180} (nmol·min/l)	55333±5164	50207±2911	90.7
hPXR	C_{max} (nmol/l)	748±45	266±7*	35.6
	AUC_{0-180} (nmol·min/l)	38064±3026	14838±493**	40.0

*P< 0.0001 compared to control.

**P= 0.0002 compared to control.

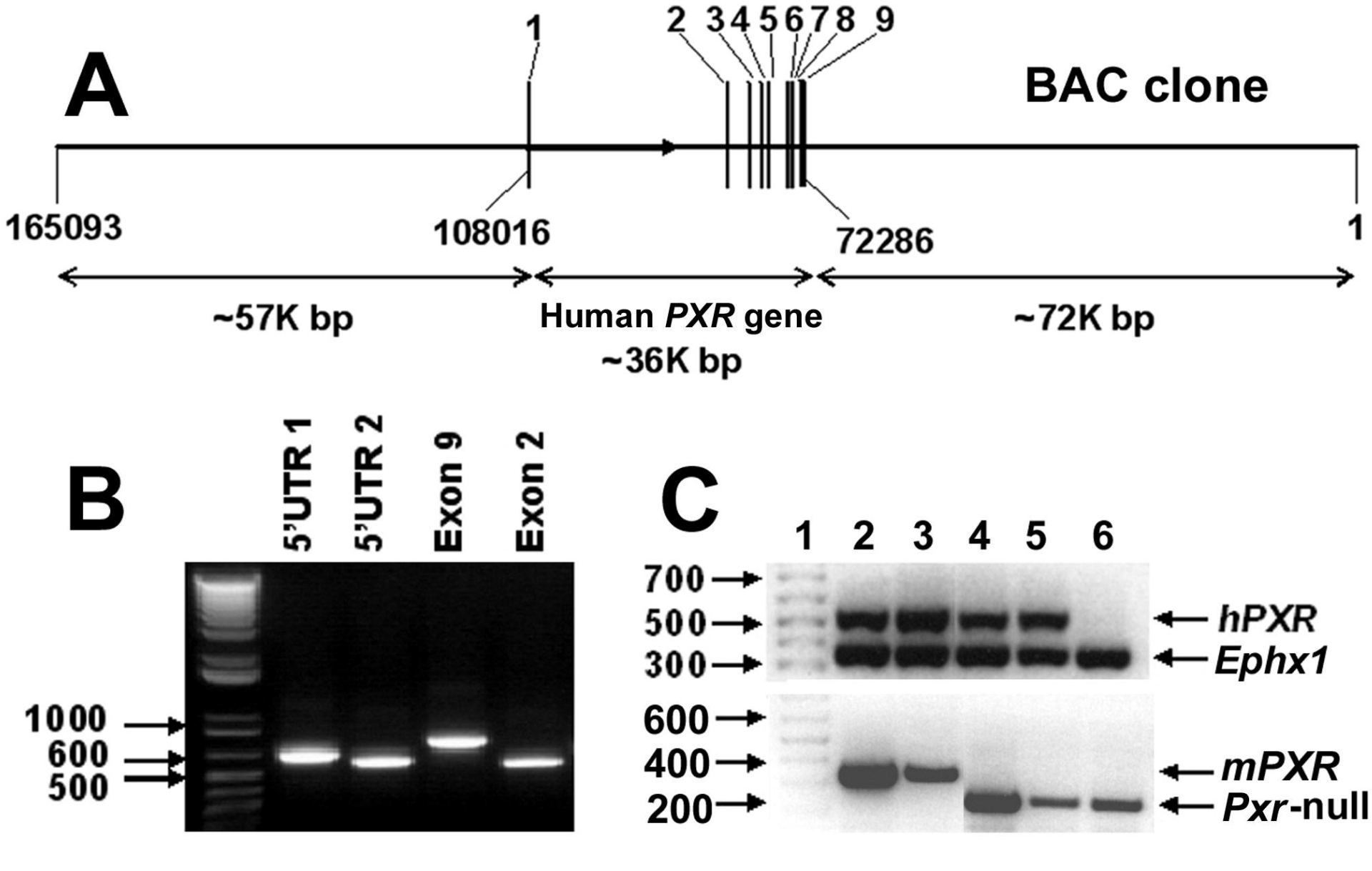
A
1
2 3 4 5 6 7 8 9
BAC clone
165093
108016
72286
1
~57K bp
Human PXR gene
~36K bp
~72K bp
B
5'UTR 1
5'UTR 2
Exon 9
Exon 2
1000
600
500
C
1 2 3 4 5 6
700
500
300
hPXR
Ephx1
600
400
200
mPXR
Pxr-null

Figure 1

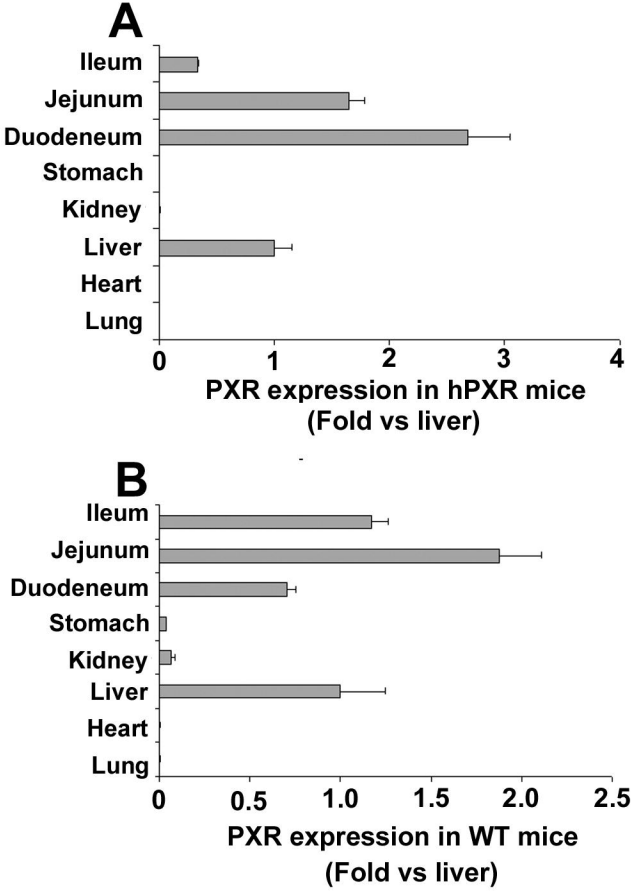
A
Ileum
Jejunum
Duodeneum
Stomach
Kidney
Liver
Heart
Lung
0
1
2
3
4
PXR expression in hPXR mice
(Fold vs liver)
B
Ileum
Jejunum
Duodeneum
Stomach
Kidney
Liver
Heart
Lung
0
0.5
1.0
1.5
2.0
2.5
PXR expression in WT mice
(Fold vs liver)

Figure 2

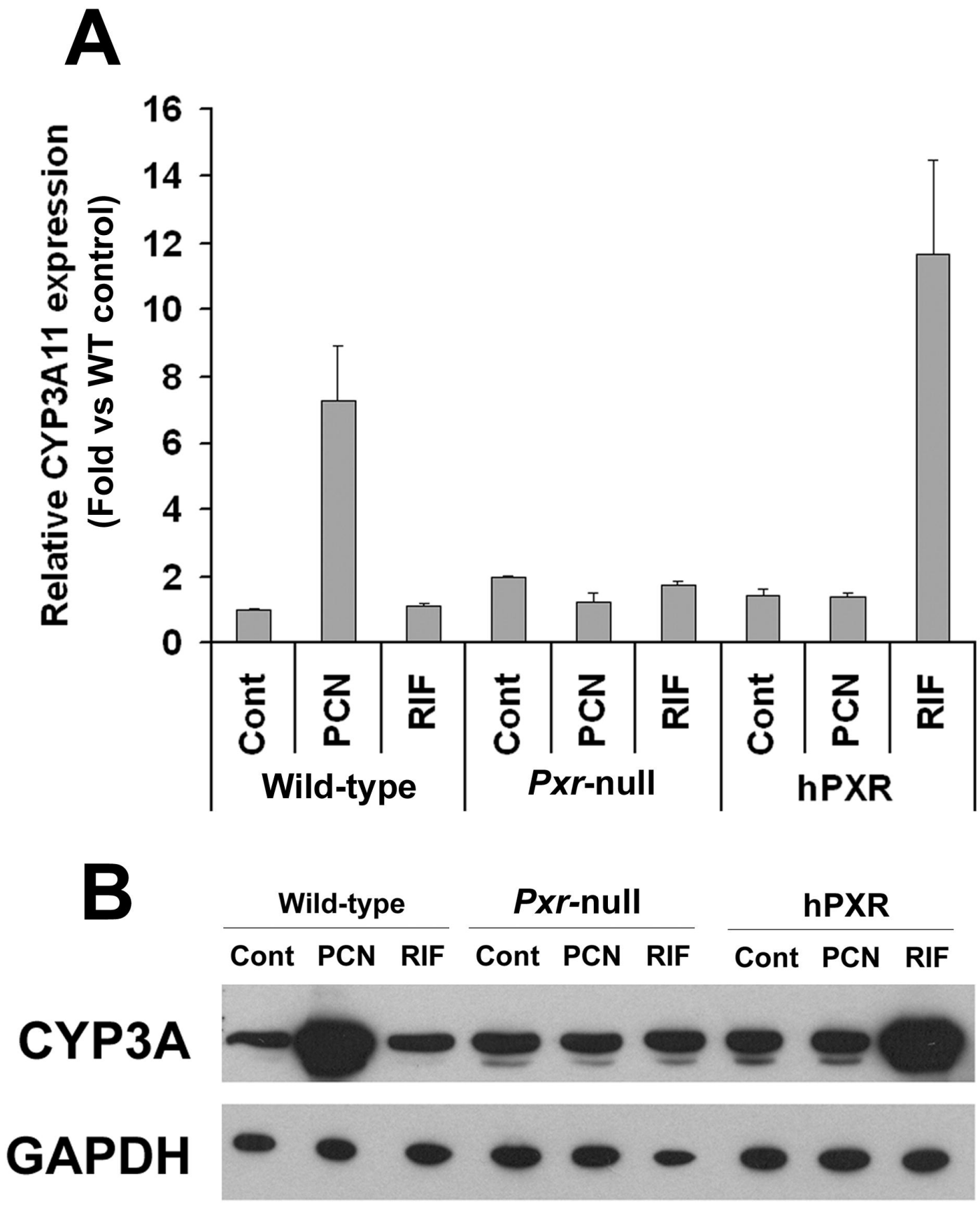
A
Relative CYP3A11 expression
(Fold vs WT control)
16
14
12
10
8
6
4
2
0
Cont
PCN
RIF
Cont
PCN
RIF
Cont
PCN
RIF
Wild-type
Pxr-null
hPXR
B
Wild-type
Pxr-null
hPXR
Cont PCN RIF Cont PCN RIF Cont PCN RIF
CYP3A
GAPDH

Figure 3

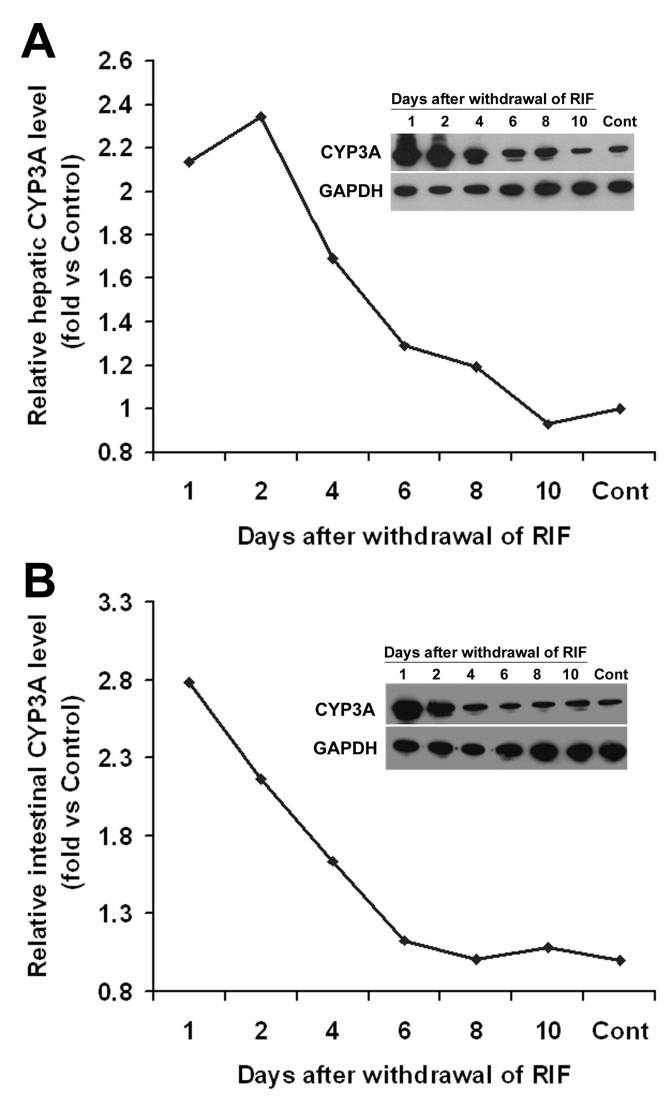
A
Relative hepatic CYP3A level (fold vs Control)
2.6
2.4
2.2
2
1.8
1.6
1.4
1.2
1
0.8
Days after withdrawal of RIF
1 2 4 6 8 10 Cont
CYP3A
GAPDH
1 2 4 6 8 10 Cont
Days after withdrawal of RIF
B
Relative intestinal CYP3A level (fold vs Control)
3.3
2.8
2.3
1.8
1.3
0.8
Days after withdrawal of RIF
1 2 4 6 8 10 Cont
CYP3A
GAPDH
1 2 4 6 8 10 Cont
Days after withdrawal of RIF

Figure 4

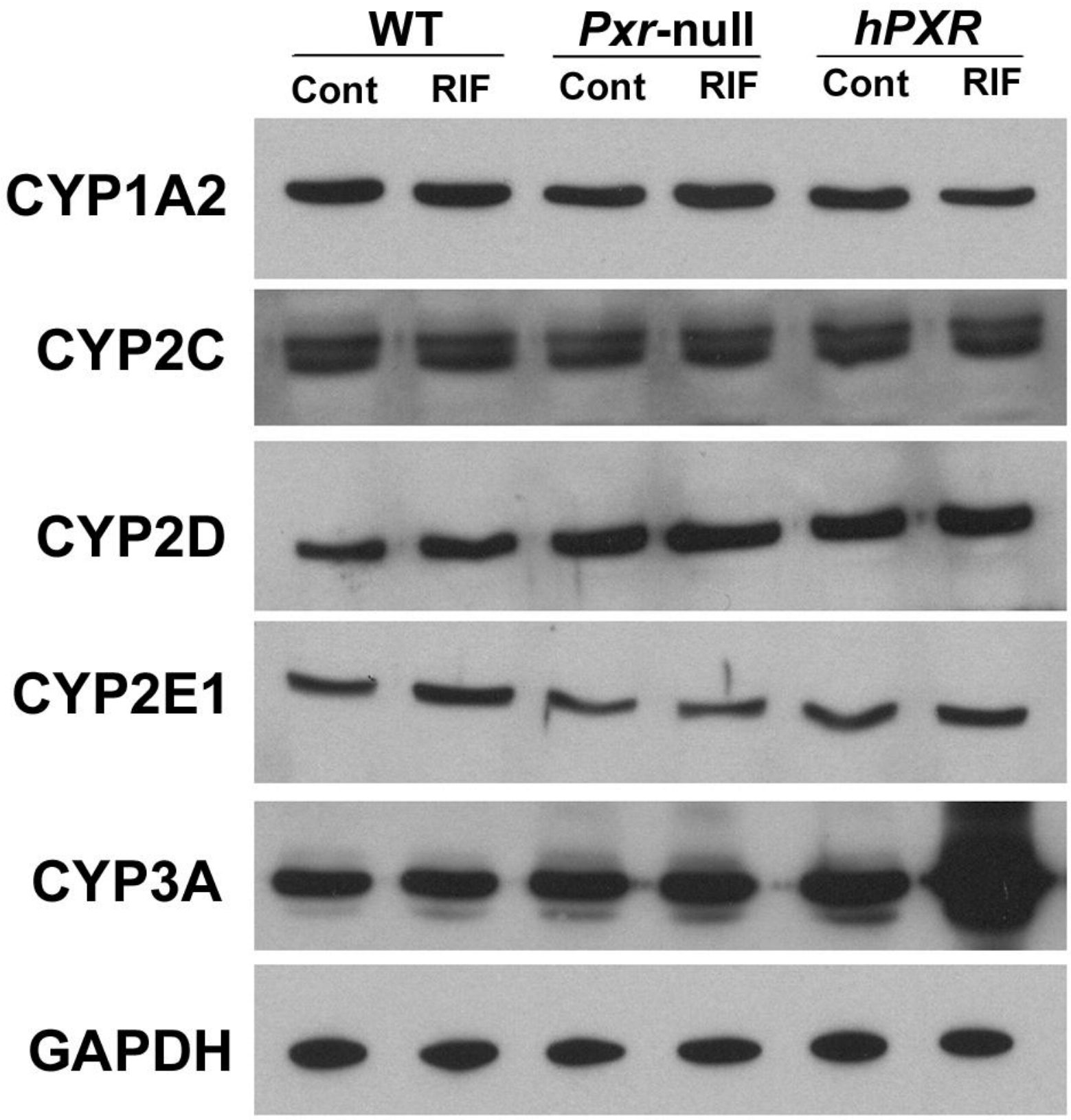
WT
Pxr-null
hPXR
Cont
RIF
Cont
RIF
Cont
RIF
CYP1A2
CYP2C
CYP2D
CYP2E1
CYP3A
GAPDH

Figure 5

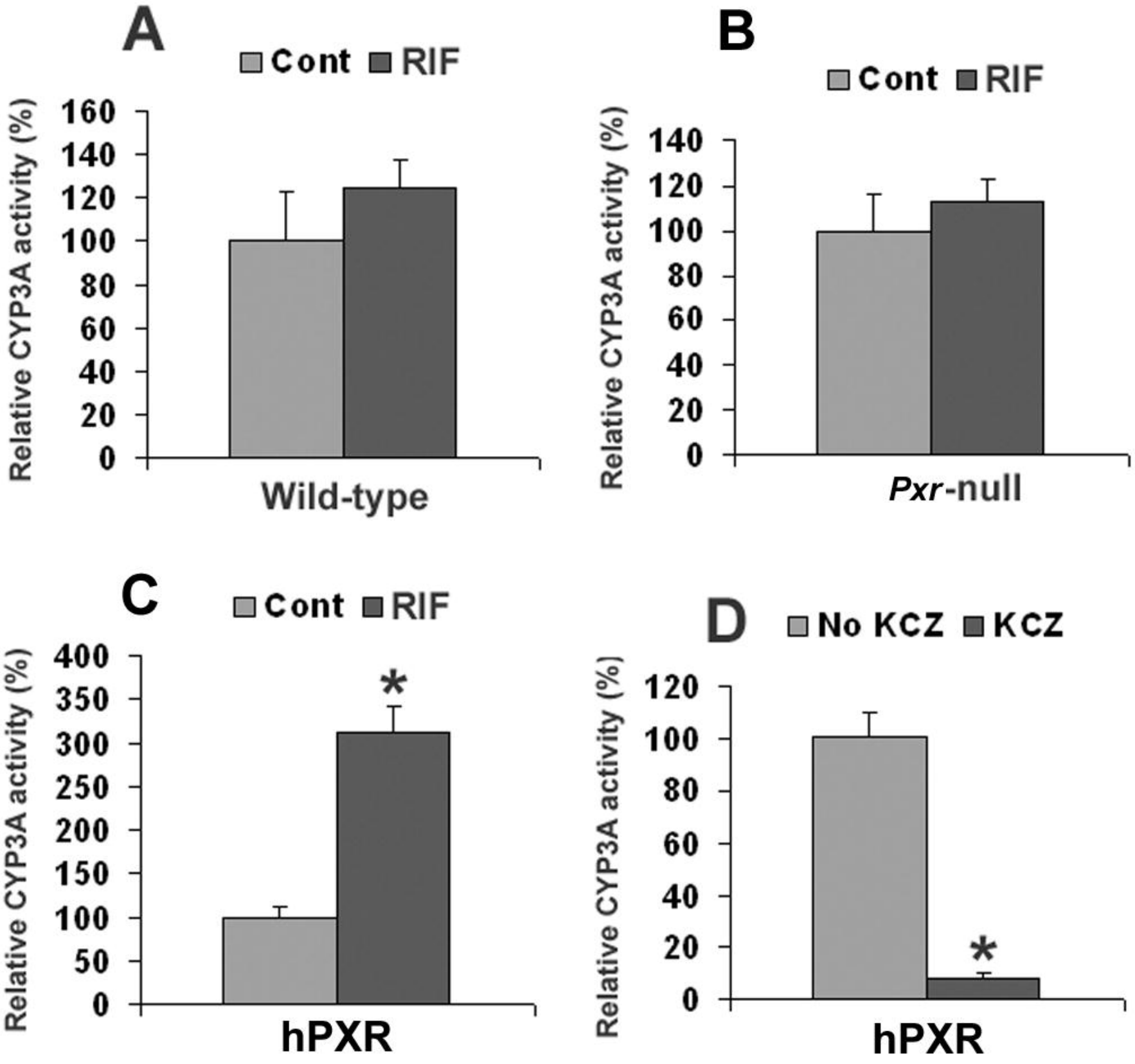
A
Cont
RIF
Relative CYP3A activity (%)
160
140
120
100
80
60
40
20
0
Wild-type
B
Cont
RIF
Relative CYP3A activity (%)
140
120
100
80
60
40
20
0
Pxr-null
C
Cont
RIF
Relative CYP3A activity (%)
400
350
300
250
200
150
100
50
0
*
hPXR
D
No KCZ
KCZ
Relative CYP3A activity (%)
120
100
80
60
40
20
0
*
hPXR

Figure 6

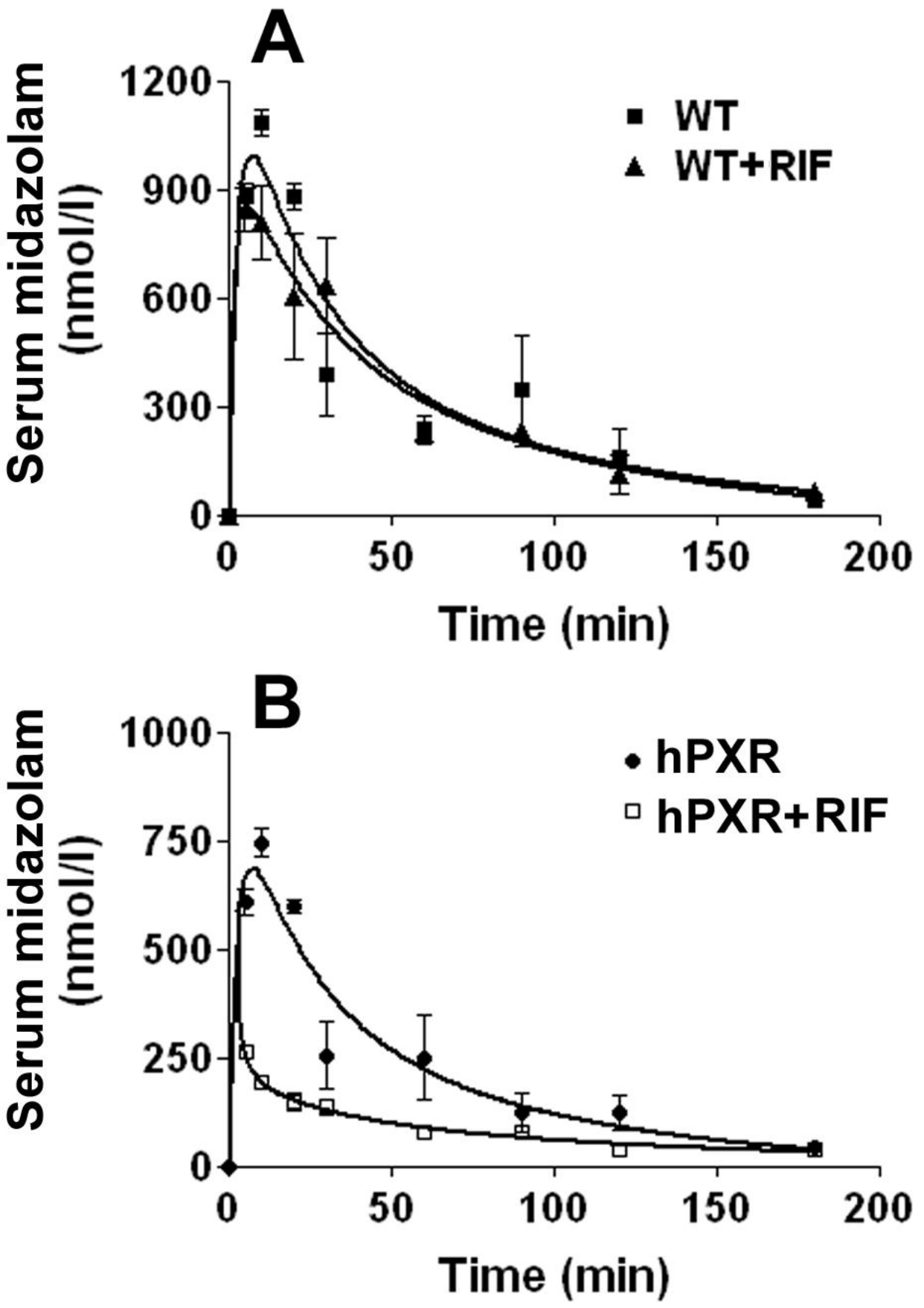
A
Serum midazolam (nmol/l)
1200
900
600
300
0
0
50
100
150
200
Time (min)
WT
WT+RIF
B
Serum midazolam (nmol/l)
1000
750
500
250
0
0
50
100
150
200
Time (min)
hPXR
hPXR+RIF

Figure 7